ASEAN Journal of Chemical Engineering 2026, Vol. 26, No. 1, 131 – 144

Microwave-Assisted Sustainable Extraction and Characterization of Chitosan from *Hermetia illucens*

Zainal Mustakim [1,2]
Agus Prasetya [1]
Joko Wintoko [1]
Fanny Sakinah [1]
Chandra Wahyu Purnomo *[,1]

[1] *Chemical Engineering Department, Engineering Faculty, Gadjah Mada University, Jl. Grafika No 2, Bulaksumur, Yogyakarta 55281, Indonesia*
[2] *Chemical Engineering Department, Engineering Faculty, Universitas Muhammadiyah Gresik, Jl. Sumatera No 101, Gresik, East Java, 61121, Indonesia*
*e-mail: chandra.purnomo@ugm.ac.id

Submitted 20 May 2025 *Revised* 31 December 2025 *Accepted* 19 March 2026

Abstract. Chitosan is a biopolymer of significant industrial interest due to its versatile physicochemical properties and wide range of applications. In line with sustainability and circular-economy principles, alternative non-crustacean sources, such as the black soldier fly *(Hermetia illucens),* have attracted increasing attention. In this study, chitosan was extracted from *H. illucens* using microwave irradiation applied to all three main processing stages: demineralization, deproteinization, and deacetylation. The performance of this approach was compared with that of conventional thermal extraction. Structural and physicochemical properties of the resulting chitosan were characterized using Fourier-transform infrared spectroscopy (FTIR), X-ray diffraction (XRD), scanning electron microscopy coupled with energy-dispersive X-ray spectroscopy (SEM–EDS), and particle size analysis (PSA). The microwave-assisted process achieved 76.01% deacetylation in 24 minutes, whereas the conventional method required 6 hours to reach a comparable 76.48%. This substantial reduction in processing time demonstrates the potential of microwave-assisted extraction as a more time- and energy-efficient approach for valorizing *H. illucens*–derived biowaste.

Keywords: Chitosan, Extraction, *Hermetia illucens*, Microwave, Waste Valorization

INTRODUCTION

Chitosan is a biopolymer derived from the deacetylation of chitin. It has attracted significant attention due to its biodegradability, non-toxicity, and biocompatibility, which enable its wide applications in agriculture, pharmaceuticals, food preservation, and environmental remediation (Mulyati *et al.,* 2023; Widarti *et al.,* 2023). Conventionally, chitosan is produced from crustacean shells; however, growing concerns about sustainability and resource availability have spurred exploration of alternative and renewable sources. In this context, the black soldier fly *(Hermetia illucens)* has emerged as a promising non-crustacean source of chitin and chitosan, supporting circular bioeconomy principles by valorizing organic waste streams (Escobar

DOI: 10.22146/ajche.21666

Rodríguez *et al.,* 2025; Mersmann *et al.,* 2025).

H. illucens larvae efficiently convert a wide range of organic wastes into valuable biomass and have been reported to generate substantially lower greenhouse gas emissions compared to conventional waste treatment methods (Hoc *et al.*, 2019; Khayrova *et al.,* 2019). Their availability across the life cycle and high chitin content during early developmental stages further strengthen their potential as a sustainable feedstock for chitosan production (Siddiqui *et al.,* 2024). Nevertheless, conventional chitosan extraction methods rely heavily on prolonged thermal treatment, resulting in high energy consumption and extended processing times (Khayrova *et al.*, 2021).

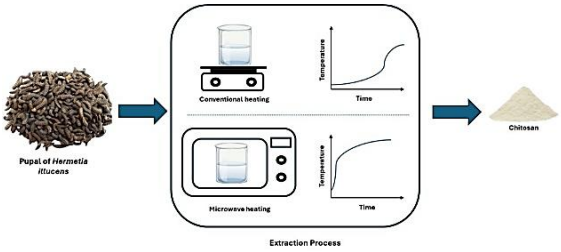


Fig. 1: Schematic of chitosan extracted from the pupal of *H. illucens*

Microwave irradiation has emerged as an effective alternative heating strategy, offering rapid and volumetric energy transfer that significantly accelerates chemical reactions while reducing energy demand (Horikoshi *et al.,* 2023; Pérez-Martínez *et al.,* 2020). In chitosan production, microwave-assisted processes have been predominantly applied during the deacetylation stage to enhance reaction efficiency. However, the application of microwave irradiation throughout all stages of extraction remains largely unexplored. Therefore, this study investigates the use of microwave irradiation during demineralization, deproteinization, and deacetylation for the extraction of chitosan from *H. illucens*. The novelty of this work lies in the full-stage integration of microwave-assisted processing, which yields chitosan of comparable quality with drastically reduced processing time, offering a rapid, environmentally friendly approach to insect-derived chitosan production.

MATERIALS AND METHOD

Materials

The raw material used in this study consisted of *H. illucens pupal*, reared at the Agrotechnology Innovation Center, Universitas Gadjah Mada (UGM), Yogyakarta, Indonesia. Commercial chitosan with an approximate degree of deacetylation of 75% was obtained from Sigma-Aldrich. All chemical reagents, including hydrochloric acid (37%), acetic acid, and sodium hydroxide, were also procured from Sigma-Aldrich.

Methods

Chitosan extraction

Chitosan was extracted from the pupal of *H. illucens* using two heating methods: conventional thermal heating and microwave-assisted heating (Figure 1). The extraction process consisted of three sequential steps: demineralization, deproteinization, and deacetylation, conducted under identical chemical conditions for both methods to enable direct comparison.

Extraction was performed in two independent batches (n = 2) for each method. Each batch was processed separately, starting from raw material preparation. Before extraction, the pupal of *H. illucens* were washed with distilled water, oven-dried, ground, and sieved to obtain particles ≤ 100 µm.

Conventional thermal extraction

The demineralization was conducted for 2 hours at 50°C with constant stirring at 200 rpm, using a raw material-to-3 M hydrochloric acid (HCl) ratio of 1:10 (w/v) (Sari *et al.,* 2024). The extracted materials were subsequently filtered and thoroughly rinsed with distilled water until the pH reached neutrality. They were then oven-dried at 60 °C overnight to eliminate residual moisture (Iñiguez-Moreno *et al.,* 2024).

Deproteinization was performed by alkaline treatment with 2 M sodium hydroxide (NaOH) at a solid-to-liquid ratio of 1:10 (w/v). The mixture was continuously stirred at 200 rpm and maintained at 80 °C for 2 hours to effectively remove protein content (Rehman *et al.,* 2023). Following the reaction, the mixture was filtered and thoroughly washed with distilled water to eliminate any residual NaOH. The resulting sample was then oven-dried at 60 °C overnight to ensure complete moisture removal.

The deproteinized material underwent deacetylation using a 12 M sodium hydroxide (NaOH) solution at 100 °C for 2 hours, with a solid-to-liquid ratio of 1:20 (w/v) and continuous stirring at 200 rpm (Triunfo *et al.,* 2022). Upon completion of the reaction, the material was thoroughly rinsed with distilled water. The solid residue was then separated from the reaction mixture by filtration or centrifugation. To achieve a neutral pH, the residue was repeatedly washed with distilled water. Finally, the product was oven-dried at 60 °C overnight to attain a consistent, dry form (Iñiguez-Moreno *et al.,* 2024).

Microwave-assisted extraction

Microwave-assisted extraction followed the same extraction sequence and chemical conditions as the conventional method, with microwave irradiation applied as the heating source. The process was conducted in a glass beaker placed inside a household microwave oven (Electrolux EMG23K22B) operating at 800 W.

To determine the optimal microwave-assisted condition, solvent contact times of 4, 6, 8, and 10 min were evaluated. The degree of deacetylation (DD%) was used as the selection criterion, and the contact time that yielded a DD comparable to that obtained with conventional heating was selected for further comparison.

Purification of chitosan

The deacetylated material obtained from each independent extraction batch was dissolved in 1% (v/v) acetic acid under continuous stirring at room temperature for 24 h (Triunfo *et al.,* 2022). The solution was centrifuged at 6,000 rpm for 15 min, and the supernatant was collected. Chitosan was precipitated by adjusting the pH to alkaline conditions using 6 M NaOH and incubated overnight at 4 °C (Das *et al.,* 2025; Triunfo *et al.,* 2022). The precipitate was recovered by centrifugation, washed repeatedly with distilled water, freeze-dried, and stored at room temperature.

Film formation

Film preparation was carried out using chitosan obtained from the independent extraction batches. Briefly, 0.1 g of chitosan was dissolved in 10 mL of 1% (v/v) acetic acid, cast onto a 100 mm polystyrene Petri dish, and dried in a desiccator for three days (Gürbüz *et al.,* 2024; Hahn *et al.,* 2020).

Characterization of chitosan

The structural and physicochemical properties of the extracted chitosan were comprehensively characterized using a suite of analytical techniques, including Fourier

Transform Infrared Spectroscopy (FTIR), X-ray Diffraction (XRD), Scanning Electron Microscopy combined with Energy-Dispersive X-ray Spectroscopy (SEM-EDS), and Particle Size Analysis (PSA).

The FTIR spectra of the chitosan samples were obtained using a Shimadzu FTIR spectrophotometer operating in attenuated total reflectance (ATR) mode over a wavenumber range of 500–4000 cm^{-1}. A total of 45 scans were accumulated at a spectral resolution of 4 cm^{-1} to ensure high-accuracy spectral analysis. The degree of deacetylation (DD%) was determined by measuring the absorbance ratio of the amide I band at 1655 cm^{-1} to the hydroxyl band at 3450 cm^{-1}, which served as an internal standard (Islam *et al.*, 2023). The degree of deacetylation (DD%) was determined from the relative absorbance of characteristic functional groups, as described below, using a reported method (Domszy and Roberts, 1985).

$$DD\% = 100 - \left[\left(\frac{A_{1655}}{A_{3450}}\right) x \frac{100}{1.33}\right] \quad (1)$$

An XRD analysis was conducted to investigate the crystalline structure of chitosan, a key parameter that influences its functional properties. This technique was used to evaluate the degree of crystallinity in the chitosan samples. The relative crystallinity was quantified as the ratio of the area under the crystalline peaks to the total area under the diffraction curve, providing a quantitative assessment of the material's crystalline content (Abdou *et al.,* 2008).

SEM-EDS analysis was employed to examine the surface morphology and microstructural characteristics of the chitosan samples. This technique enables high-resolution imaging at extreme magnifications, facilitating the detailed visualization of surface features. Additionally, EDS enables qualitative and semi-quantitative elemental analysis, offering insights into the material's composition and the presence of residual elements or impurities (Hayes *et al.,* 2019). SEM-EDS analysis was conducted to assess the structural integrity, surface texture, and elemental distribution of the synthesized chitosan.

Particle Size Analysis comprises a set of techniques for measuring the size, shape, and distribution of particles within a given sample. In this study, PSA was utilized to determine the particle size distribution of the chitosan samples, providing valuable information on their physical characteristics and suitability for various applications.

Data analysis

Quantitative extraction data are presented as mean ± SD from two independent extraction batches (n = 2). Material characterization analyses were conducted once per sample and are therefore reported descriptively without statistical testing, as the study focuses on comparative process evaluation rather than hypothesis-based analysis.

RESULTS AND DISCUSSION

Chitosan Yield

The extraction of chitosan from *H. illucens* using microwave irradiation has attracted increasing attention for sustainable waste valorization and resource-efficient processing. Microwave-assisted extraction (MAE) has been reported to enhance mass transfer and reaction kinetics through rapid, and volumetric heating, thereby reducing processing time compared with conventional thermal methods (El Knidri *et al.,* 2016; Lertjindaporn *et al.,* 2025).

In the present study, the effectiveness of MAE was evaluated by comparing impurity removal efficiencies at each extraction stage with those obtained using the conventional method. For the conventional process, demineralization, deproteinization, and deacetylation removed 53.10 ± 10.04%, 67.50 ± 0.71%, and 88.60 ± 0.14% of impurities, respectively. In contrast, the MAE approach achieved higher removal efficiencies of 56.80 ± 3.15%, 87.54 ± 0.73%, and 90.56 ± 0.08%, respectively. These trends are consistent with previous studies reporting enhanced reaction efficiency under microwave irradiation due to improved reagent penetration and accelerated reaction kinetics (El Knidri *et al.*, 2016; Siddiqui *et al.*, 2024).

The resulting chitosan yield was 3.28 ± 0.35% for the conventional method and 3.89 ± 2.35% for the MAE process. These values fall within the range reported for *H. illucens*-derived chitosan (2–8%), as obtained using formic acid demineralization and alkaline deproteinization followed by deacetylation (Triunfo *et al.,* 2022). Although slightly lower than yields typically reported for crustacean sources (approximately 4–15%), the results are consistent with previous findings that insect-derived chitosan generally exhibits lower extractable fractions due to differences in cuticle composition and mineral content (Coltelli *et al.*, 2025).

While direct energy consumption was not measured in this study, previous work has demonstrated that microwave-assisted deacetylation can substantially reduce energy demand, from 382.1 to 8.9 kJ g^{-1} of chitosan, compared with conventional heating (Bruno *et al.,* 2024). This literature-based evidence supports the potential of MAE as a more energy-efficient approach, consistent with the shorter processing time observed in the present work.

FTIR Analysis

The degree of deacetylation (DD%) was estimated from FTIR spectra, and the results are presented in Figure 2. A microwave irradiation time of approximately 8 min produced a DD value comparable to that obtained using the conventional method. The reported DD values represent representative measurements from single experimental runs and are intended for qualitative comparison of process performance. Similar trends have been reported in previous studies, indicating that microwave irradiation can substantially shorten the deacetylation process while maintaining comparable levels of chemical conversion (Bruno *et al.,* 2024).

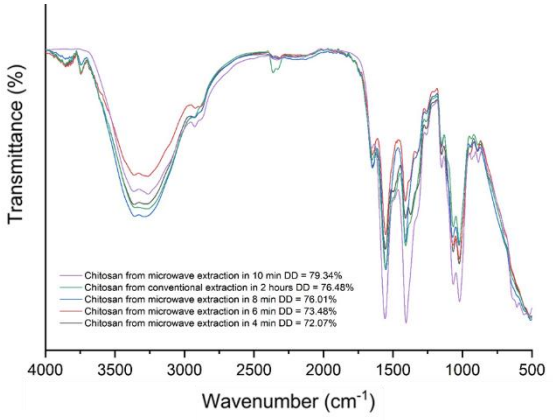


Fig. 2: FTIR spectra of chitosan extracted using microwave and conventional methods

The microwave-assisted process reduced the total extraction time from 6 h to 24 min while yielding comparable DD values of 76.01% and 76.48% for microwave-assisted and conventionally extracted chitosan, respectively. This represents an approximately fifteen-fold reduction in processing time. Although direct energy consumption was not quantified in this study, the markedly shorter processing duration supports the potential of microwave-assisted extraction as a more time-efficient approach, consistent with previous reports highlighting its improved

energy efficiency for chitosan production.

Figure 3 shows the FTIR spectra of chitosan films obtained by microwave-assisted extraction, conventional extraction, and commercial reference. All spectra exhibit the characteristic absorption features of chitosan, confirming successful deacetylation regardless of the extraction route. The broad absorption band in the region of 3600–3200 cm^{-1} is attributed to overlapping O–H and N–H stretching vibrations, reflecting extensive intra- and intermolecular hydrogen bonding within the polymer network (Jadoon *et al.*, 2022). The bands observed at 2960–2878 cm^{-1} correspond to C–H stretching vibrations of aliphatic groups (Ruiz Matute *et al.*, 2013).

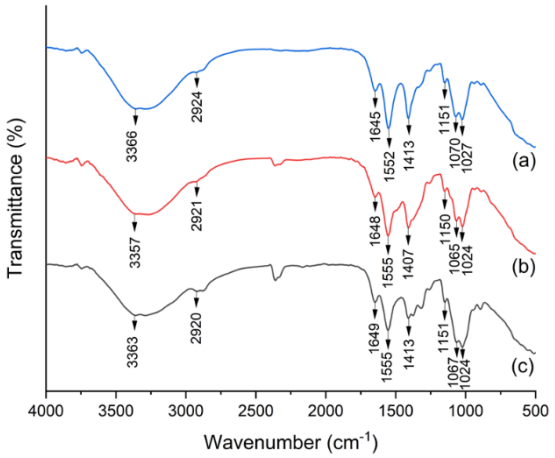


Fig. 3: FTIR spectra of chitosan films obtained by (a) microwave-assisted extraction, (b) conventional extraction, and (c) commercial chitosan, showing characteristic functional groups of chitosan.

The absorption bands located at approximately 1645, 1552, and 1413 cm^{-1} are assigned to amide I (C=O stretching), amide II (N–H bending), and amide III (C–N stretching coupled with N–H bending), respectively *(*Kumar *et al., 2021;* Triunfo *et al.*, 2022). These bands are directly related to the acetylated and deacetylated functional groups of chitosan and thus indicate the degree of deacetylation. The comparable relative intensities of these bands in microwave-assisted and conventionally extracted samples suggest that both methods achieve a similar extent of acetyl group removal.

Characteristic polysaccharide vibrations were also observed at approximately 1153 cm^{-1}, corresponding to the asymmetric stretching of the C–O–C bridge in the glycosidic linkage, while bands near 1070 and 1027 cm^{-1} are attributed to C–OH stretching vibrations of the polysaccharide ring of chitosan (Kumar *et al.*, 2021; Pădureţu *et al.*, 2019). The presence of these peaks across all samples confirms the preservation of the polysaccharide backbone during extraction. Minor variations in peak intensity among samples are likely associated with differences in hydrogen-bonding interactions and local molecular ordering induced by the distinct heating mechanisms.

Overall, the FTIR analysis demonstrates that microwave-assisted extraction does not alter the fundamental chemical structure of chitosan and produces functional group features comparable to those of conventionally extracted and commercial chitosan.

XRD Analysis

The crystalline structure of chitosan films was examined using X-ray diffraction, and the corresponding diffractograms are shown in Figure 4. All samples exhibit diffraction features characteristic of semi-crystalline chitosan, indicating the coexistence of ordered crystalline domains and amorphous regions within the polymer matrix.

Distinct diffraction peaks were observed at 2θ values of approximately 38.26°, 44.46°, 64.83°, and 77.82° for all samples, reflecting the presence of crystalline domains formed

through intermolecular interactions among chitosan chains. In addition, the conventionally extracted chitosan showed additional peaks at 2θ ≈ 13.91°, 16.76°, and 25.38°, indicating a higher degree of molecular ordering than in the microwave-assisted and commercial samples. Peaks near 2θ ≈ 20° are commonly associated with hydrated or partially crystalline chitosan and are sensitive to processing history, solvent interactions, and drying conditions (Qiao *et al.*, 2021; Rahmi *et al.,* 2024).

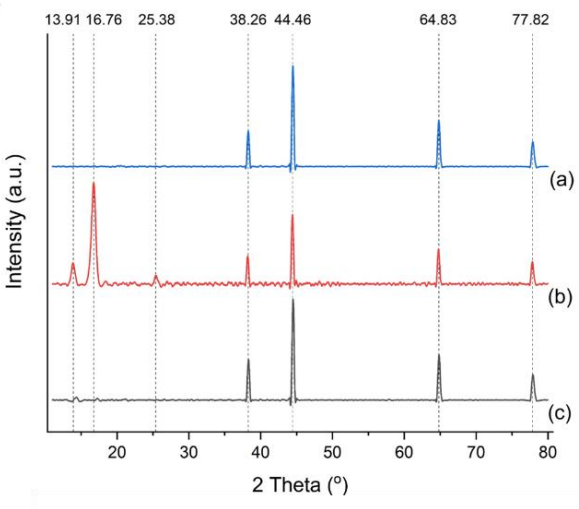


Fig. 4: XRD patterns of chitosan films obtained by (a) microwave-assisted extraction, (b) conventional extraction, and (c) commercial chitosan, showing the characteristic semi-crystalline structure of chitosan.

The calculated crystalline indices were 37.76% for conventionally extracted chitosan, 20.33% for microwave-assisted chitosan, and 19.35% for commercial chitosan. The higher crystallinity observed for the conventionally processed sample can be attributed to prolonged thermal exposure, which allows polymer chains to rearrange into more ordered conformations. In contrast, microwave irradiation provides rapid volumetric heating that may disrupt intermolecular hydrogen bonding and limit chain realignment, thereby reducing crystallinity.

Crystallinity in chitosan is strongly influenced by the degree of deacetylation and the availability of free amino ($–NH_2$) groups, which promote intermolecular hydrogen bonding and facilitate ordered chain packing (Li *et al.,* 2020; Margret, A. A., Begum, T., & Kumar, 2017). Although the DD values of the samples are comparable, slight differences in heating mechanism and molecular mobility can lead to variations in crystalline ordering. The semi-crystalline nature observed for all samples is consistent with previous reports on insect-derived chitosan (Qashqoosh *et al.,* 2019; Triunfo *et al.,* 2022).

From a functional perspective, differences in crystallinity may influence physicochemical behavior such as solubility, flexibility, and film-forming performance. Lower crystallinity, as observed in microwave-assisted chitosan, is often associated with enhanced chain mobility and processability, whereas higher crystallinity is associated with improved rigidity and structural stability (Ferreira *et al.,* 2020). These findings indicate that microwave-assisted processing not only reduces extraction time but also enables modulation of chitosan structural organization, which may be advantageous for tailoring material properties toward specific applications.

SEM-EDS Analysis

The surface morphology and microstructural features of chitosan films were examined using scanning electron microscopy (SEM), as shown in Figure 5. Chitosan obtained via microwave-assisted extraction, conventional extraction, and commercial sources all exhibit irregular,

porous, and microfibrillar surface structures, which are characteristic of chitosan-based materials. Similar morphologies have been widely reported for chitosan derived from crustacean and insect sources, where partial disruption of the native chitin matrix during deproteinization and deacetylation leads to fibrillar and porous architectures (Dong *et al.*, 2023; Triunfo *et al.*, 2022).

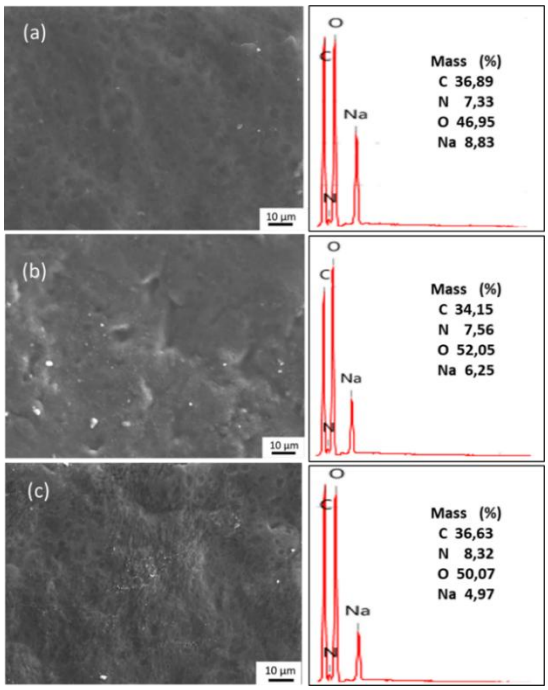


Fig. 5: SEM images (left) showing surface morphology and EDS spectra (right) showing elemental composition of chitosan obtained by (a) microwave-assisted extraction, (b) conventional extraction, and (c) commercial chitosan.

Notably, differences in surface compactness and pore distribution are observable among the samples. The microwave-assisted chitosan displays a relatively more homogeneous and less compact morphology, which may be attributed to rapid volumetric heating during microwave treatment. Such heating promotes faster solvent penetration and limits polymer chain rearrangement, resulting in a looser network structure with increased surface porosity. Similar effects have been reported for microwave-assisted extraction of chitosan and other biopolymers, where accelerated heating reduces crystallite growth and promotes more open microstructures (Poppi *et al.,* 2022).

In contrast, chitosan obtained via conventional thermal extraction exhibits denser and more compact surface regions. Prolonged heating under conventional conditions facilitates molecular rearrangement and stronger intermolecular hydrogen bonding, leading to tighter packing of polymer chains. Comparable compact morphologies have been observed in chitosan extracted from shrimp shells and insect biomass under extended thermal treatment (Qashqoosh *et al.,* 2019; Triunfo *et al.,* 2022). These morphological differences are consistent with the higher crystallinity observed in the XRD analysis of conventionally extracted chitosan.

The commercial chitosan sample shows relatively uniform and smoother surface features, reflecting its industrial processing and controlled purification conditions. Such morphology is commonly reported for commercially refined chitosan products and is associated with standardized processing steps that reduce surface heterogeneity (de Farias *et al*., 2019).

Energy-dispersive X-ray spectroscopy (EDS) analysis confirms the presence of carbon (C), oxygen (O), and nitrogen (N) as the dominant elements in all samples, consistent with the chemical composition of chitosan. Minor sodium (Na) signals were also detected and are attributed to residual sodium species originating from alkaline treatment during deacetylation and neutralization, as previously reported in the literature (Lima *et al.,* 2014). No significant

qualitative differences in elemental composition were observed among the microwave-assisted, conventional, and commercial chitosan samples, indicating that the extraction method does not alter the material's elemental composition.

Particle Size Analysis

Particle size plays an important role in determining the solubility, mechanical behavior, and bioactivity of chitosan-based materials, with smaller, more uniform particles generally exhibiting improved performance (Thanakkasaranee *et al.,* 2021). The particle size distributions of chitosan obtained by different extraction methods are shown in Figure 6.

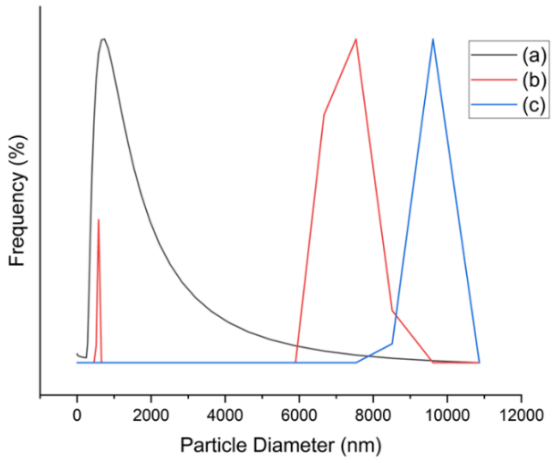


Fig. 6: Particle size distribution of chitosan obtained by (a) microwave-assisted extraction, (b) conventional extraction, and (c) commercial chitosan.

Chitosan obtained via microwave-assisted extraction exhibits a predominantly monodispersed particle size distribution, characterized by a single dominant peak at 1,135.6 ± 964.9 nm. Commercial chitosan shows a similar monodispersed profile with a peak at 8,988.7 ± 237.6 nm. In contrast, conventionally extracted chitosan displays a polydisperse distribution, evidenced by two distinct peaks at 539.4 ± 19.3 nm and 6,840.0 ± 522.8 nm. In this context, a monodispersed system refers to a narrow particle size distribution with a single dominant population. In contrast, a polydisperse system exhibits a broader or multimodal distribution, indicating greater heterogeneity in particle size.

The more uniform particle size obtained by microwave-assisted extraction can be attributed to rapid and homogeneous volumetric heating, which promotes simultaneous nucleation and limits excessive particle growth. This mechanism suppresses agglomeration and leads to a narrower size distribution (Forouzandeh *et al.,* 2022; Poppi *et al.*, 2022). In contrast, conventional heating involves slower and less uniform heat transfer, allowing prolonged particle growth prior to nucleation and resulting in broader, heterogeneous size distributions (Poppi *et al.*, 2022).

Monodispersed particle systems are generally associated with more predictable flow behavior and improved stability compared with polydisperse systems, which may exhibit complex interparticle interactions due to size variability *(*Fazli *et al.*, 2024; Seiphoori *et al.*, 2020). Therefore, the narrower particle size distribution observed for microwave-assisted chitosan suggests potential advantages for applications requiring uniformity and controlled physicochemical behavior.

CONCLUSIONS

Chitosan was successfully extracted using both conventional and microwave-assisted heating methods. The application of microwave heating significantly reduced the extraction time from 6 hours to only 24

minutes, while maintaining a comparable degree of deacetylation (DD%) to that achieved by the conventional method—76.48% and 76.01%, respectively. Structural, morphological, and chemical analyses confirmed that the chitosan obtained via microwave irradiation exhibited characteristics similar to those produced by conventional heating. Furthermore, the crystallinity of chitosan extracted by both methods closely resembled that of commercial chitosan, indicating consistent structural integrity. This environmentally friendly approach offers a fifteen-fold reduction in processing time, underscoring its potential as a more efficient and sustainable alternative to traditional extraction methods. Future research should aim to optimize further microwave parameters, such as power level, irradiation time, and temperature control, to enhance chitosan yield and quality while minimizing energy input and processing costs.

ACKNOWLEDGEMENT

This research was supported by the Ministry of Education, Culture, Research, and Technology of the Republic of Indonesia under the dissertation doctoral grant (048/E5/PG.02.00.PL/2024;2769/UN1/DITLIT/PT.01.03/2024).

DECLARATION OF COMPETING INTEREST

The authors declare that they have no known competing financial interests or personal relationships that could have influenced the content or findings of this paper.

REFERENCES

Abdou, E.S., Nagy, K.S.A., and Elsabee, M.Z., 2008. "Extraction and characterization of chitin and chitosan from local sources." *Bioresour. Technol., 99*, 1359–1367. https://doi.org/10.1016/j.biortech.2007.01.051

Bruno, M., Silva, D.O., Oliveira, S.A. De, and Rosa, S., 2024. "Comparative study on microwave-assisted and conventional chitosan production from shrimp shell : Process optimization, characterization, and environmental impacts." *J. Clean. Prod., 440*, 140726. https://doi.org/10.1016/j.jclepro.2024.140726

Coltelli, M.-B., Gigante, V., Panariello, L., Aliotta, L., Scieuzo, C., Falabella, P., and Lazzeri, A., 2025. "Chitin and chitosan materials from black soldier fly (*Hermetia Illucens*): An insight onto their thermal degradation and mechanical behavior linked to their copolymeric structure." *Polym. Test., 150*, 108922. https://doi.org/10.1016/j.polymertesting.2025.108922

Das, P., Das, M., Sahoo, S.K., Dandapat, J., and Pradhan, J., 2025. "Characterization of extracellular chitin deacetylase from Aneurinibacillus aneurinilyticus isolated from marine crustacean shell." *Curr. Res. Microb. Sci., 8*, 100325. https://doi.org/10.1016/j.crmicr.2024.100325

de Farias, B.S., Sant'Anna Cadaval Junior, T.R., and de Almeida Pinto, L.A., 2019. "Chitosan-functionalized nanofibers: A comprehensive review on challenges and prospects for food applications." *Int. J. Biol. Macromol., 123*, 210–220. https://doi.org/10.1016/j.ijbiomac.2018.11.042

Domszy, J.G., and Roberts, G.A.F., 1985. "Evaluation of infrared spectroscopic techniques for analysing chitosan." *Die Makromol. Chemie., 186*, 1671–1677. https://doi.org/10.1002/macp.1985.021860815

Dong, Q., Qiu, W., Feng, Y., Jin, Yingshan, Deng, S., Tao, N., and Jin, Yinzhe, 2023. "Proteases and microwave treatment on the quality of chitin and chitosan produced from white shrimp (Penaeus vannamei)." *eFood, 4*. https://doi.org/10.1002/efd2.73

El Knidri, H., El Khalfaouy, R., Laajeb, A., Addaou, A., and Lahsini, A., 2016. "Eco-friendly extraction and characterization of chitin and chitosan from the shrimp shell waste via microwave irradiation." *Process Saf. Environ. Prot., 104*, 395–405. https://doi.org/10.1016/j.psep.2016.09.020

Escobar Rodríguez, C., Zaremska, V., Klammsteiner, T., Kampatsikas, I., Münstermann, N., Weichold, O., and Gruber, S., 2025. "Chitosan obtained from black soldier fly larval cuticles expands the value chain and is effective as a biocontrol agent to combat plant pathogens." *Carbohydr. Polym., 349*, 123023. https://doi.org/10.1016/j.carbpol.2024.123023

Fazli, M., Rudman, M., Kuang, S., and Chryss, A., 2024. "Predicting bidisperse particle settling from mono-sized settling systems." *Powder Technol., 437*, 119545. https://doi.org/10.1016/j.powtec.2024.119545

Ferreira, D.C.M., de Souza, A.L., da Silveira, J.V.W., Pelissari, F.M., Marim, B.M., Giraldo, G.A.G., Mantovan, J., and Mali, S., 2020. "Chitosan nanocomposites for food packaging applications", in Multifunctional Hybrid Nanomaterials for Sustainable Agri-food and Ecosystems, Elsevier. https://doi.org/10.1016/B978-0-12-821354-4.00017-0

Forouzandeh, P., Ganguly, P., Dahiya, R., and Pillai, S.C., 2022. "Supercapacitor electrode fabrication through chemical and physical routes." *J. Power Sources, 519*, 230744. https://doi.org/10.1016/j.jpowsour.2021.230744

Gürbüz, Z., Şengül, M., Erkaya-Kotan, T., and Sarıcaoğlu, F.T., 2024. "A novel composite edible film based on quince seed gel and whey protein concentrate as affected by transglutaminase crosslinking." *Int. J. Food Sci. Technol., 59*, 6163–6173. https://doi.org/10.1111/ijfs.17350

Hahn, T., Roth, A., Ji, R., Schmitt, E., and Zibek, S., 2020. "Chitosan production with larval exoskeletons derived from the insect protein production." *J. Biotechnol., 310*, 62–67. https://doi.org/10.1016/j.jbiotec.2019.12.015

Hayes, E., Cnuts, D., and Rots, V., 2019. "Integrating SEM-EDS in a sequential residue analysis protocol: Benefits and challenges." *J. Archaeol. Sci. Reports, 23*, 116–126. https://doi.org/10.1016/j.jasrep.2018.10.029

Hoc, B., Noël, G., Carpentier, J., Francis, F., and Megido, R.C., 2019. "Optimization of BSF artificial reproduction." *PLoS One 14*, 1–13.

Horikoshi, S., Mura, H., and Serpone, N., 2023. "Three-dimensional observations of the electric field distribution of variable frequency microwaves, and scaling-up organic syntheses." *Commun. Chem., 6*. https://doi.org/10.1038/s42004-023-

01062-6

Iñiguez-Moreno, M., Santiesteban-Romero, B., Melchor-Martínez, E.M., Parra-Saldívar, R., and González-González, R.B., 2024. "Valorization of fishery industry waste: Chitosan extraction and its application in the industry." *MethodsX, 13*. https://doi.org/10.1016/j.mex.2024.102892

Islam, M.M., Islam, R., Mahmudul Hassan, S.M., Karim, M.R., Rahman, M.M., Rahman, S., Nur Hossain, M., Islam, D., Aftab Ali Shaikh, M., and Georghiou, P.E., 2023. "Carboxymethyl chitin and chitosan derivatives: Synthesis, characterization and antibacterial activity." *Carbohydr. Polym. Technol., Appl. 5*, 100283. https://doi.org/10.1016/j.carpta.2023.100283

Jadoon, A., Ali, Z., Farooq, W.A., Ali, F., Price, G.J., Taimur, S., Atif, M., AlMutairi, M.A., Yaqub, N., and Bibi, S., 2022. "Probing the role of hydrolytically stable, 3-aminopropyl triethoxysilane crosslinked chitosan/graphene oxide membrane towards Congo red dye adsorption." *Curr. Appl. Phys., 40*, 110–118. https://doi.org/10.1016/j.cap.2021.07.006

Khayrova, A., Lopatin, S., and Varlamov, V., 2021. "Obtaining and study of physicochemical properties of chitin/chitosan-melanin complexes from Hermetia illucens." *J. Phys. Conf. Ser., 1942*, 0–6. https://doi.org/10.1088/1742-6596/1942/1/012003

Khayrova, A., Lopatin, S., and Varlamov, V., 2019. "Black Soldier Fly Hermetia illucens as a Novel Source of Chitin and Chitosan." *Int. J. Sci., 8*, 81–86. https://doi.org/10.18483/ijsci.2015

Kumar, S., Ye, F., Mazinani, B., Dobretsov, S., and Dutta, J., 2021. "Chitosan nanocomposite coatings containing chemically resistant zno–snox core–shell nanoparticles for photocatalytic antifouling." *Int. J. Mol. Sci., 22*. https://doi.org/10.3390/ijms22094513

Lertjindaporn, M., Geng, J.T., Keratimanoch, S., Lee, G.Y., Ryo, K., and Osako, K., 2025. "Chitin and chitosan from North Pacific krill (Euphausia Pacifica): Comparative study of conventional and microwave-assisted extraction methods and the potential use in chitosan film production." *Int. J. Biol. Macromol., 296*, 139692. https://doi.org/10.1016/j.ijbiomac.2025.139692

Li, B., Elango, J., and Wu, W., 2020. "Recent advancement of molecular structure and biomaterial function of chitosan from marine organisms for pharmaceutical and nutraceutical application." *Appl. Sci., 10*, 30–50. https://doi.org/10.3390/app10144719

Lima, H.A., Lia, F.M.V., and Ramdayal, S., 2014. "Preparation and Characterization of Chitosan-Insulin-Tripolyphosphate Membrane for Controlled Drug Release: Effect of Cross Linking Agent." *J. Biomater. Nanobiotechnol. 05*, 211–219. https://doi.org/10.4236/jbnb.2014.54025

Margret, A. A., Begum, T., & Kumar, A.G., 2017. "Discerning the potential of chitosan extracted from bio resources as a competent brain drug carrier to cross the blood brain barrier." *Indian J. Pharm. Sci., 79*.

Mersmann, L., Gomes, V., Souza, L., and Fernando, A.L., 2025. "Green Processes for chitin and chitosan production from

insects : current state , challenges , and opportunities.", *Polymers, 17(9),* 1185; https://doi.org/10.3390/polym17091185

Mulyati, S., Rosnelly, C.M., Syamsuddin, Y., Arahman, N., Muchtar, S., Wahyuni, Lauzia, T., Ambarita, A.C., Bilad, M.R., and Samsuri, S., 2023. "Enhancing the anti-fouling property of polyethersulfonebased membrane using chitosan additive from golden snail (*Pomacea canaliculata*) shell waste for water purification." *ASEAN J. Chem. Eng., 23*, 224–239. https://doi.org/10.22146/ajche.79643

Pădurețu, C.C., Isopescu, R.D., Gîjiu, C.L., Rău, I., Apetroaei, M.R., and Schröder, V., 2019. "Optimization of chitin extraction procedure from shrimp waste using Taguchi method and chitosan characterization." *Mol. Cryst. Liq. Cryst., 695*, 19–28. https://doi.org/10.1080/15421406.2020.1723902

Pérez-Martínez, B.T., Aboudzadeh, M.A., Schubert, U.S., Leiza, J.R., and Tomovska, R., 2020. "Microwave irradiation versus conventional heating assisted free-radical copolymerization in solution." *Chem. Eng., J. 399*, 125761. https://doi.org/10.1016/j.cej.2020.125761

Poppi, G., Colombini, E., Salvatori, D., Balestri, A., Baldi, G., Leonelli, C., and Veronesi, P., 2022. "A multi-physic modelling insight into the differences between microwave and conventional heating for the synthesis of TiO_2 nanoparticles." *Processes, 10 (4),* 697. https://doi.org/10.3390/pr10040697

Qashqoosh, M.T.A., Alahdal, F.A.M., Manea, Y.K., Zakariya, S.M., and Naqvi, S., 2019. "Synthesis, characterization and spectroscopic studies of surfactant loaded antiulcer drug into Chitosan nanoparticles for interaction with bovine serum albumin." *Chem. Phys., 527*, 110462. https://doi.org/10.1016/j.chemphys.2019.110462

Qiao, C., Ma, X., Wang, X., and Liu, L., 2021. "Structure and properties of chitosan films: Effect of the type of solvent acid." *Lwt, 135*, 109984. https://doi.org/10.1016/j.lwt.2020.109984

Rahmi, Harnila, Lubis, S., Julinawati, Mustafa, I., and MZ, K., 2024. "Fabrication of Glycine-Chitosan/TiO_2 film for metanil yellow removal from water." *South African J. Chem. Eng., 47*, 254–261. https://doi.org/10.1016/j.sajce.2023.12.002

Rehman, K. ur, Hollah, C., Wiesotzki, K., Heinz, V., Aganovic, K., Rehman, R. ur, Petrusan, J.I., Zheng, L., Zhang, J., Sohail, S., Mansoor, M.K., Rumbos, C.I., Athanassiou, C., and Cai, M., 2023. "Insect-derived chitin and chitosan: a still unexploited resource for the edible insect sector." *Sustainability, 15 (6),* 4864. https://doi.org/10.3390/su15064864

Ruiz Matute, A.I., Cardelle-Cobas, A., García-Bermejo, A.B., Montilla, A., Olano, A., and Corzo, N., 2013. "Synthesis, characterization and functional properties of galactosylated derivatives of chitosan through amide formation." *Food Hydrocoll., 33*, 245–255. https://doi.org/10.1016/j.foodhyd.2013.03.016

Sari, I.P., Mulatsari, E., Mumpuni, E., and Purwanggana, A., 2024. "The demineralization optimization for chitosan synthesis from crab shell waste (*Portunus pelagicus*)." *JOPS J. Pharm. Sci.,*

7, 73–77. https://doi.org/10.36341/jops.v7i2.4653

Seiphoori, A., Ma, X. guang, Arratia, P.E., and Jerolmack, D.J., 2020. "Formation of stable aggregates by fluid-assembled solid bridges." *Proc. Natl. Acad. Sci., U. S. A. 117*, 3375–3381. https://doi.org/10.1073/pnas.1913855117

Siddiqui, S.A., Greunen, L. van, Zeiri, A., Yudhistira, B., Ahmad, A., and Monnye, M., 2024. "The potential of chitin and chitosan from dead black soldier fly (BSF) (*Hermetia illucens*) for biodegradable packaging material – A critical review." *Process Saf. Environ. Prot., 189*, 1342–1367. https://doi.org/10.1016/j.psep.2024.06.108

Thanakkasaranee, S., Jantanasakulwong, K., Phimolsiripol, Y., Leksawasdi, N., Seesuriyachan, P., Chaiyaso, T., Jantrawut, P., Ruksiriwanich, W., Sommano, S.R., Punyodom, W., Reungsang, A., Ngo, T.M.P., Thipchai, P., Tongdeesoontorn, W., and Rachtanapun, P., 2021. "High substitution synthesis of carboxymethyl chitosan for properties improvement of carboxymethyl chitosan films depending on particle sizes." *Molecules, 26*. https://doi.org/10.3390/molecules26196013

Triunfo, M., Tafi, E., Guarnieri, A., Salvia, R., Scieuzo, C., Hahn, T., Zibek, S., Gagliardini, A., Panariello, L., Coltelli, M.B., De Bonis, A., and Falabella, P., 2022. "Characterization of chitin and chitosan derived from Hermetia illucens, a further step in a circular economy process." *Sci. Rep., 12*, 1–17. https://doi.org/10.1038/s41598-022-10423-5

Widarti, S., Suprianti, Y., Kurniasetiawati, A.S., and Tritjahjono, R.I., 2023. "The efficiency of κ-Carrageenan-Chitosan-PVA-MWCNTs membranes in removing methylene blue, rhodamine b, bromocresol purple, and murexid from water." *ASEAN J. Chem. Eng., 23*, 282–289. https://doi.org/10.22146/ajche.78794